Coupling interaction between a single emitter and the propagating surface plasmon polaritons in a graphene microribbon waveguide*

Zhang Lei(张 磊)[a], Fu Xiu-Li(符秀丽)[a]†, Lei Ming(雷 鸣)[a], Chen Jian-Jun(陈建军)[a], Yang Jun-Zhong(杨俊忠)[a], Peng Zhi-Jian(彭志坚)[b], and Tang Wei-Hua(唐为华)[a]‡

[a] *School of Science, Beijing University of Posts and Telecommunications, Beijing* 100876, *China*
[b] *School of Engineering and Technology, China University of Geosciences, Beijing* 100083, *China*

(Received 7 June 2013; revised manuscript received 6 August 2013; published online 14 January 2014)

The coupling interaction between an individual optical emitter and the propagating surface plasmon polaritons in a graphene microribbon (GMR) waveguide is investigated by numerical calculations, where the emitter is situated above the GMR or in the same plane of the GMR. The results reveal a multimode coupling mechanism for the strong interaction between the emitter and the propagating plasmonic waves in graphene. When the emitter is situated in the same plane of the GMR, the decay rate from the emitter to the surface plasmon polaritons increases more than 10 times compared with that in the case with the emitter above the GMR.

Keywords: graphene, coupling interaction, surface plasmon polariton

PACS: 81.05.ue, 42.25.Dd, 52.40.Db **DOI:** 10.1088/1674-1056/23/3/038101

1. Introduction

Surface plasmon polaritons (SPPs), the electromagnetic waves coupled to charge oscillations at a noble metal–dielectric interface, have attracted considerable attention for their strong confinement of electromagnetic fields on a sub-wavelength scale,[1–5] which makes them uniquely viable to realize nano-photonics. However, a major obstacle to realize this great dream is the enormous loss of photons when the noble metals are working in the frequency regimes of interest. However, recent intensive research studies on the plasmon in graphene have shown that SPPs in graphene[6,7] have higher confinement in volume,[8] longer propagation length,[9] and tunability of the plasmonic properties by electrical or chemical modification.[10,11] The SPPs can also affect the behavior of graphene, such as the doping level.[12] So graphene has been considered as a better candidate for novel photonic and optoelectronic applications, such as photodetectors,[13–15] optical sensing,[16,17] and waveguides.[7,9,18]

As is well known, all of these photonic and optoelectronic applications rely on the interaction of photons with graphene. For example, the interaction between a single emitter and the propagating photon fields will determine whether the quantum information from the emitter can be propagated for a long distance in the waveguides,[19,20] which is essential for quantum communication. In the literature, Koppens *et al.*[8] demonstrated the interactions between a single emitter and SPPs in an infinite graphene sheet and between a single emitter and a localized surface plasmon (SP) in graphene nano-ribbons, however no reports can be found on the interaction between a single emitter and propagating SPPs in a one-dimensional graphene waveguide where the quantum information can propagate in a specific direction. There is an investigation on the interaction between SPPs in paired graphene ribbons,[21] however the interaction between an emitter and SPPs has not been reported. So, in the present paper, we investigate the coupling interaction between an individual optical emitter and the propagating SPPs in a graphene microribbon (GMR) waveguide, where the emitter is situated above the GMR or in the same plane of the GMR. By modeling the decay rates of the emitter polarized along different directions, the coupling mechanism between the emitter and the propagating plasmonic waves in graphene is discussed. The results reported here might be helpful for manipulating the light–graphene interaction on a nanoscale.

2. Simulations and analyses

The structures to be investigated are shown in Figs. 1(a) and 1(b). The GMR is situated in the *xoy* plane and the ribbon center line is placed at the *oy* axis. In Fig. 1(a), the emitter is situated in the *yoz* plane and 50 nm above the center line of the GMR, named the out-of-plane excitation. In Fig. 1(b), the emitter is situated in the *xoy* plane and 50 nm away from the GMR edge, called the in-plane excitation. For simplicity, it is assumed that the GMR is surrounded by air. For numerical calculations, the random-phase approximation[22,23] is used in the local limit for the conductivity σ of graphene at zero tem-

*Project supported by the National Natural Science Foundation of China (Grant Nos. 51172030, 11274052, 51102019, 51172208, and 61274015) and the National Basic Research Program of China (Grant No. 2010CB923200).

†Corresponding author. E-mail: xiulifu@bupt.edu.cn
‡Corresponding author. E-mail: whtang@bupt.edu.cn

© 2014 Chinese Physical Society and IOP Publishing Ltd

perature, which can be taken as

$$\sigma(\omega) = \frac{e^2 E_{\mathrm{F}}}{\pi\hbar^2}\frac{\mathrm{i}}{\omega + \mathrm{i}\tau^{-1}} + \frac{e^2}{4\hbar}\left[\theta(\hbar\omega - 2E_{\mathrm{F}}) + \frac{\mathrm{i}}{\pi}\log\left|\frac{\hbar\omega - 2E_{\mathrm{F}}}{\hbar\omega + 2E_{\mathrm{F}}}\right|\right], \quad (1)$$

where the Fermi level E_{F} of graphene is chosen to be 0.2 eV, and the relaxation time is $\tau = 5 \times 10^{-13}$ s as measured in Refs. [24] and [25] for non-impurity graphene. Both the SPP mode analysis and the three-dimensional (3D) simulation of the coupling between the emitter and the SPPs in the GMR are conducted by using the finite-element commercial software COMSOL. In addition, as surface plasmons are the collective excitations of the total free electronic charge, the structure of graphene edges, no matter whether it is armchair or zigzag, would not change the coupling interaction,[16] so in this work, the effect of the graphene edge morphology is not taken into consideration in the calculation.

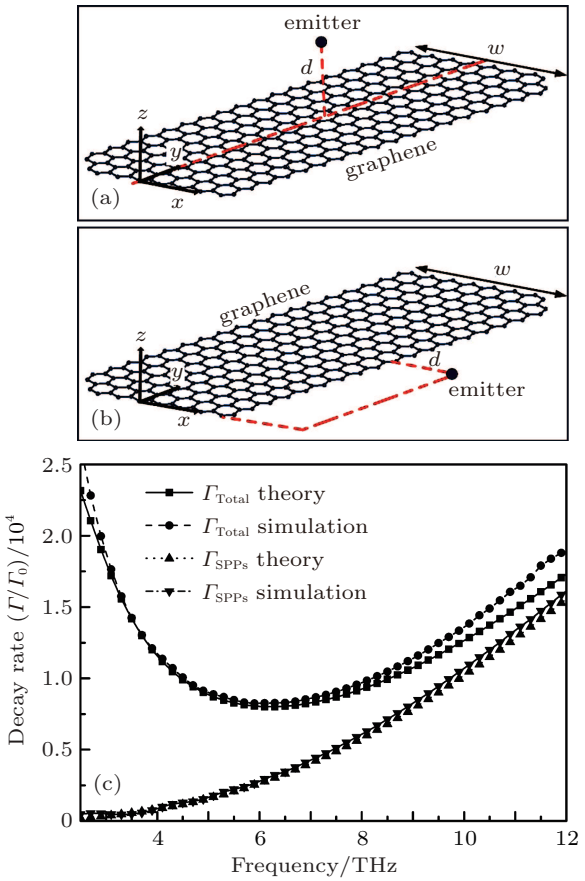


Fig. 1. (color online) Sketches of our simulations for (a) out-of-plane excitation, where the emitter is located above the GMR, and (b) in-plane excitation, where the emitter is situated in the same plane as the GMR. (c) Theoretically calculated and simulated decay rates of the emitter to an infinite graphene sheet.

Moreover, full 3D finite-element simulations are also performed to obtain the decay rate of the emitter in front of an infinite graphene mono-layer sheet. According to Ref. [8], for the emitter polarized in the direction perpendicular to the graphene sheet, its total decay rate can be theoretically calculated as

$$\Gamma_{\mathrm{Total}} \approx \Gamma_0 + \frac{4}{\hbar}|p|^2\int_0^{\infty} k_{//}^2\,\mathrm{d}k_{//} \times \mathrm{Im}\left(\frac{-1}{2 + 4\pi\mathrm{i}k_{//}\sigma/\omega}\right)\mathrm{e}^{-2k_{//}z}, \quad (2)$$

where $k_{//}$ is the wave vector parallel to the graphene sheet, p is the transition dipole matrix for the emitter, Γ_0 is the decay rate of the emitter in vacuum, and the contribution to Γ_{Total} from the SPPs can be expressed as

$$\Gamma_{\mathrm{SPPs}} \approx \frac{2\pi^4}{\hbar}|p|^2\frac{\mathrm{e}^{-4\pi z/\lambda_{\mathrm{SPPs}}}}{\lambda_{\mathrm{SPPs}}^3}. \quad (3)$$

For simulations, the emitter is taken as an electric dipole, the thickness of graphene is taken to be 0.5 nm, and the dipole–graphene separation is assumed to be $d = 50$ nm. The total decay rate is derived by calculating the total energy flowing out of the dipole, and the decay rates for the SPPs are obtained by calculating the energy flowing into the direction in which the SPPs propagate. The simulated results are then compared with the theoretically calculated ones based on Eqs. (2) and (3), which is shown in Fig. 1(c). The good agreement between these two series of data (Γ_{Total} and Γ_{SPPs}) verifies the correctness of the simulation method in this work.

Figure 2(a) presents the typical numerically simulated results for both Γ_{Total} and Γ_{SPPs} of the emitter situated 50 nm above the GMR as shown in Fig. 1(a), with a width of 5 μm and $E_{\mathrm{F}} = 0.2$ eV. From this figure, it can be seen that for both Γ_{Total} and Γ_{SPPs}, their change trends with frequency in the GMR are similar to those in the infinite graphene sheet shown in Fig. 1(c). Besides, the Γ_{SPPs} shows a step-like shape with the frequency no matter whether the emitter is polarized along the x or z direction, which may result from the multi-mode coupling between the emitter and the SPPs in the GMR. As shown in the relation between the real part of the effective refraction index ($N_{\text{eff-r}}$, defined as $\lambda_0/\lambda_{\mathrm{SPPs}}$) and the frequency (Fig. 3(a)) with the help of COMSOL, there are a variety of propagating modes at different frequencies. The SPP propagation length is very short when nearly being banned (i.e., when $N_{\text{eff-r}}$ is close to 1) and can exceed tens of the lifetimes when the SPPs are far from being banned.[16] The near electric-field intensities and the field directions for the modes indicated by numbers 1–6 in Fig. 3(a) are plotted in Fig. 3(b). According to the characteristics of the electric field profiles, the propagating modes of the SPPs in the GMR can be divided into symmetric modes with odd mode numbers and anti-symmetric modes with even mode numbers. When the emitter is polarized along the x direction, it only interacts with the anti-symmetric modes, i.e., modes 2, 4, and 6; for the case with the z polarization, it interacts with the symmetric modes,

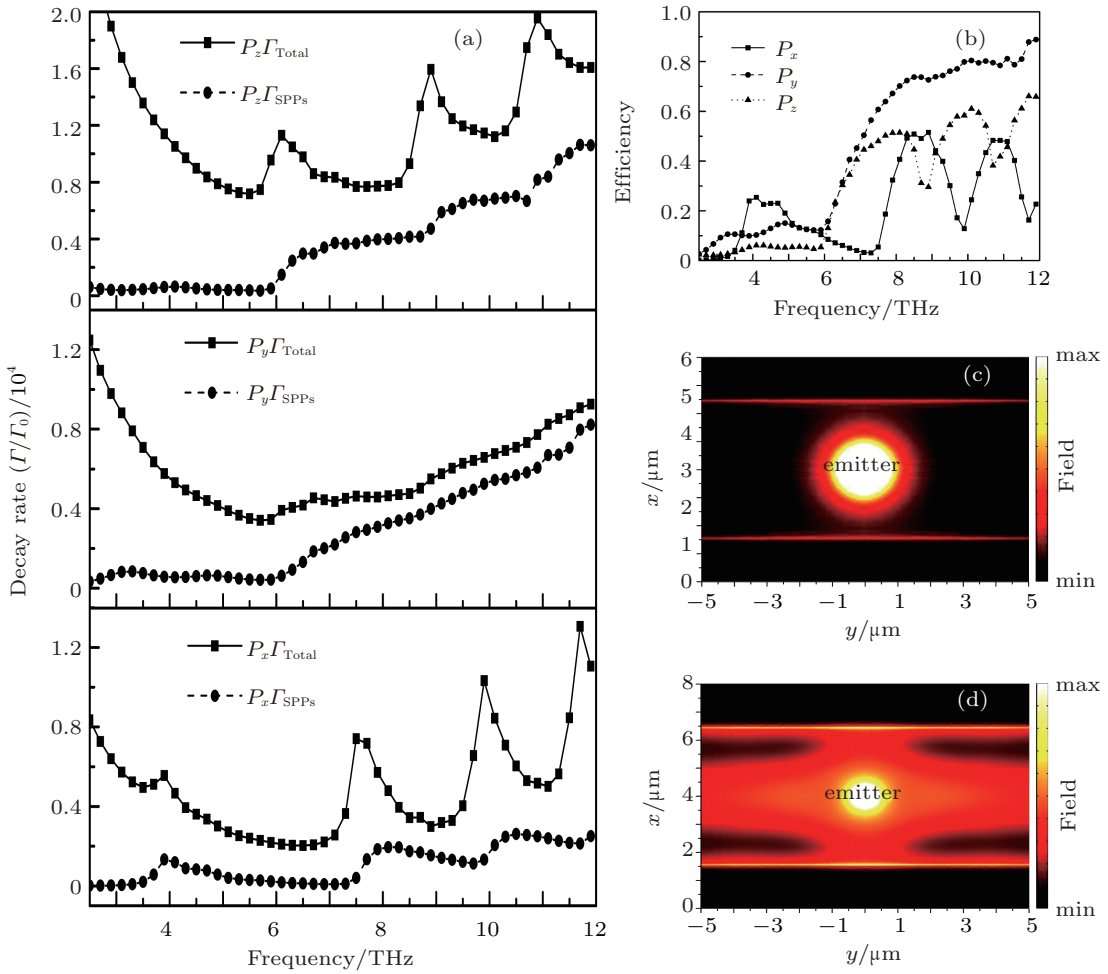


Fig. 2. (color online) (a) Simulated variations of $\Gamma_{\rm Total}$ and $\Gamma_{\rm SPPs}$ of the emitter polarized along x, y, and z directions with frequency for the out-of-plane excitations, where the emitter is placed 50 nm above the GMR with 5 μm in width and Fermi energy $E_{\rm F} = 0.2$ eV. (b) Coupling efficiencies for the emitter at three different polarizations. Normalized 3D electrical field profiles at exciting frequencies $f_{\rm exc}$ of (c) 2.5 THz and (d) 8 THz with the emitter polarized in the z direction.

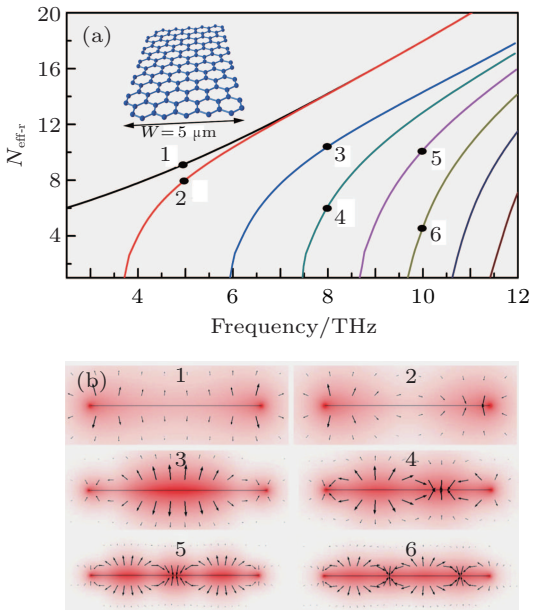


Fig. 3. (color online) (a) Dispersion curves of propagating SPP modes in the GMR with 5 μm in width. (b) Near electric-field intensities and field directions of the modes corresponding to labels 1–6 in panel (a). Frequencies for these modes are marked by the dots in panel (a).

i.e., modes 1, 3, and 5. Good agreement can be found between the frequencies where the steps at different polarization directions appear as shown in Fig. 2(a) and the ones where the SPP modes are banned in Fig. 3(a). Moreover, the curves of $\Gamma_{\rm Total}$ with frequency along the x and z polarizations present sharp peaks at the same frequencies where the steps of $\Gamma_{\rm SPPs}$ appear. As the propagation modes approach to being banned, the group velocity sharply decreases and the propagation loss greatly increases, which make the propagation modes strongly localized. Thus we propose that these peaks result from the localized graphene plasmon resonance (LGPR) modes.[26] On the other hand, the LGPR modes have been proved to be excited when the emitter is polarized in the cross-section (*xoz* plane) of a GMR waveguide.[8] Another fact is that there is no peak for $\Gamma_{\rm Total}$ when the emitter is polarized along the y direction, which reveals that the dipole does not interact with the LGPR under these circumstances.

Furthermore, the coupling efficiencies at three polarizations are shown in Fig. 2(b). The coupling efficiency is defined as $\Gamma_{\rm SPPs}/\Gamma_{\rm Total}$, which features the rate of photon decay-

ing into the SPP modes. With higher coupling efficiencies, more energy of the emitter will transfer to the SPP modes and less energy will be wasted in local dissipation channels. From Fig. 2(b), one can see that the efficiencies show many valleys when the emitter is polarized in the x and z directions, which is caused by the strong interaction between the emitter and the LGPR. However, the efficiency in the y polarization direction presents a smooth curve and a higher efficiency. Typical 3D electrical field profiles at a distance of 10 nm above the graphene for the emitter polarized along the z direction are shown in Figs. 2(c) and 2(d), and the exciting frequencies $f_{\rm exc}$ are set to be 2.5 THz and 8 THz respectively. It clearly reveals that the propagating field of the SPP is concentrated on the edges of the GMR at $f_{\rm exc} = 2.5$ THz as shown in Fig. 2(c), and the propagating field exists both around the edges and in the mid of the GMR at $f_{\rm exc} = 8$ THz as shown in Fig. 2(d). The high electrical field intensity around the emitter is caused by its non-radiating field. According to the above analysis, only mode 1 can be excited in the GMR at the frequency of 2.5 THz and both modes 1 and 3 exist at the frequency of 8 THz. Good agreement can also be found between the propagating field shown in Fig. 2 and the field profiles of the SPP modes in Fig. 3(b).

Figure 4(a) shows the simulated variations of $\Gamma_{\rm Total}$ and $\Gamma_{\rm SPPs}$ of the emitter polarized along the z direction with frequency for the out-of-plane excitations, where the emitter is located 50 nm above the GMR with 3 μm in width. It can be seen that compared with the emitter with a ribbon width of 5 μm discussed above, the emitter with a shorter ribbon width has an increased decay rate. This can be explained by the fact that as the ribbon width is reduced, the mode area of the SPP is also reduced, thus resulting in a small effective mode volume according to Eq. (4). Another feature is observed, with a reduced ribbon width, the resonance peaks of the emitter shift toward higher frequencies, and less peaks are observed in the frequency window. The reason is that the SPP modes in graphene have a strong dependence on the ribbon width, and the SPP dispersion relations are also changed with ribbon widths (see Fig. 4(b)). This is also proved by the good agreement between the resonance peak positions and the dispersion relations of the emitter as shown in Fig. 4. At z polarization, the dipole only interacts with the SPP modes of odd numbers (1, 3, or 5) and the frequencies of the resonance peaks are exactly consistent with the band edges of modes 3 and 5. In our work, the distance between the emitter and the graphene layer is set to be 50 nm. In fact, the gap between the emitter and the graphene layer can also affect the emitter decay rate. As the emitter approaches the graphene sheet, the field at the emitter becomes stronger, resulting in smaller effective mode volume $V_{\rm eff}$ according to Eq. (4), and thus a larger decay rate.

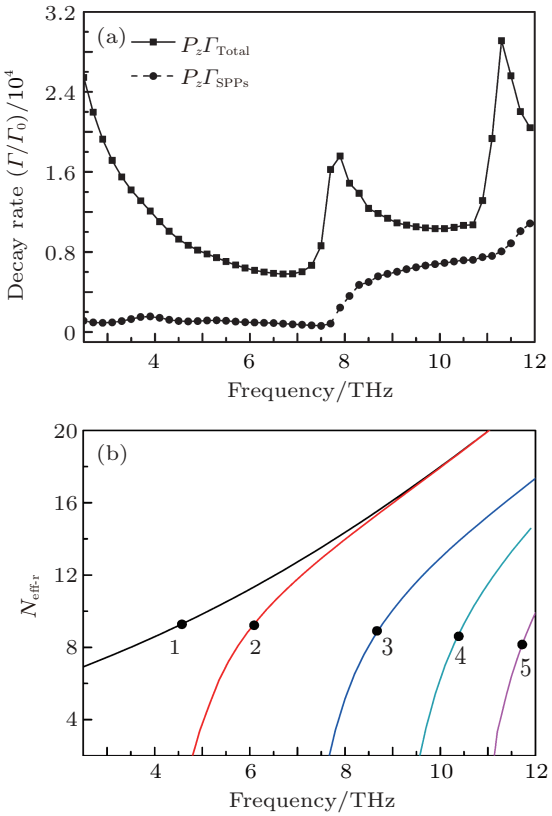


Fig. 4. (color online) (a) Simulated variations of $\Gamma_{\rm Total}$ and $\Gamma_{\rm SPPs}$ of the emitter polarized along the z direction with frequency for the out-of-plane excitations, where the emitter is located 50 nm above the GMR with 3 μm in width and Fermi energy $E_{\rm F} = 0.2$ eV. (b) Dispersion curves of propagating SPP modes in the GMR with 3 μm in width.

For the in-plane excitation shown in Fig. 1(b), the numerically simulated results of decay rates and coupling efficiencies are presented in Fig. 5. The emitter is situated in the same plane as the GMR and 50 nm away from the edge of the GMR. As the electric field in the z direction is zero as indicated in Fig. 3(b), there exists no coupling when the emitter is polarized in the z direction, and thus we only investigate the cases in which the emitter is polarized in the x and y directions. As shown in Fig. 5(a), when the emitter is polarized in the x direction, one can see that the decay rates increase more than 10 times compared to those of the out-of-plane excitations. In such a case, the emitter can interact with all propagating modes of the SPPs in the GMR, which can be inferred from the resonance peaks in $\Gamma_{\rm Total}$. The increase of the decay rate can be understood from Fermi's golden rule. As is well known, the emitter coupling strength g and the effective mode volume $V_{\rm eff}$ of GMR's SPPs are related by $g \propto (V_{\rm eff})^{1/2}$. In addition, the $V_{\rm eff}$ of the GMR can be expressed as[27]

$$V_{\rm eff} = \ell \frac{1}{2} \iint \left(\varepsilon_0 \frac{{\rm d}(\varepsilon\omega)}{{\rm d}\omega} |E(\boldsymbol{r},\omega)|^2 + \mu_0 |H(\boldsymbol{r},\omega)|^2 \right) {\rm d}\boldsymbol{r} \times (\varepsilon\varepsilon_0 |E(\boldsymbol{r}_{\rm e},\omega)|^2)^{-1}, \quad (4)$$

where ℓ is an arbitrary quantization length, $\boldsymbol{r}_{\rm e}$ is the position of the emitter, and $E(\boldsymbol{r}_{\rm e},\omega)$ is the field intensity at $\boldsymbol{r}_{\rm e}$. The integral can be viewed as the integration of electromagnetic field

power in different modes in space. When the emitter is polarized in the x direction, the electric field E_x mainly concentrates on the GMR edges, as shown in the inset of Fig. 5(a). Therefore, when the emitter is moved from the middle to the edge of the GMR, $E(\boldsymbol{r}_e, \omega)$ becomes stronger, resulting in a smaller V_{eff} and thus a higher interaction strength. As for the y polarization, the in-plane excitation result is similar to that of the out-of-plane excitation, in which the decay rate curves are still smooth and the increase of the decay rate is not obvious. The simulation results indicate that the dipole cannot interact with the LGPR with the y polarization. The coupling efficiencies for the two different polarizations are plotted in Fig. 5(b); we obtain a similar result to that in the case of out-of-plane excitation, i.e., there are many valleys for the x polarization and the curve for the y polarization is smooth.

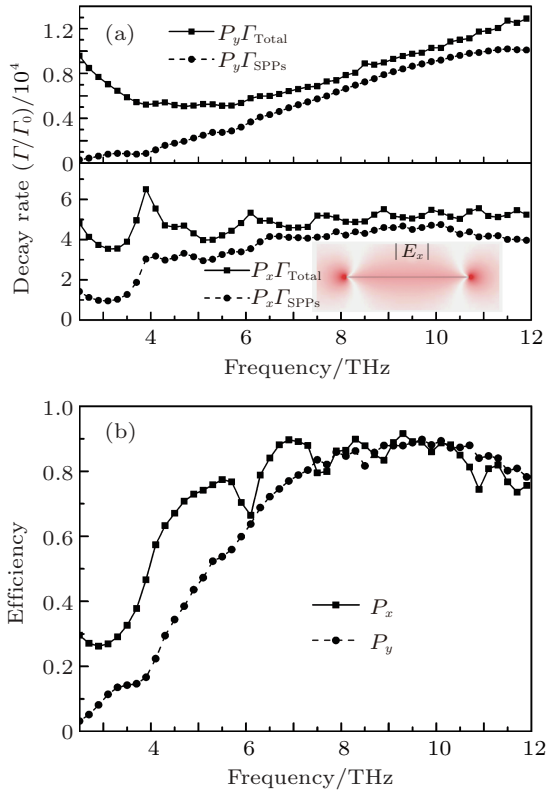


Fig. 5. (color online) (a) and (b) Simulated variations of Γ_{Total} and Γ_{SPPs} of the emitter polarized along the x and y directions with frequency for the in-plane excitations, where the emitter is situated 50 nm away from the GMR edge, the width of the GMR is 5 μm, and Fermi energy $E_F = 0.2$ eV. Inset shows the intensity profiles of the electric field in the x direction. (b) Coupling efficiencies for the emitter in the two different polarizations.

3. Conclusion

In this paper, the coupling interaction between an individual optical emitter and the propagating SPP modes in a GMR waveguide is investigated numerically, where the emitter is situated above the GMR or in the same plane of the GMR. The result reveals a multimode coupling mechanism of the strong interaction between the emitter and the propagating plasmonic waves in graphene. Furthermore, when the emitter is situated in the same plane of the GMR, the decay rate from the emitter to SPPs increases more than 10 times compared with that in the case with the emitter above the GMR. The results might be useful in manipulating the interaction of photons with graphene.

References

[1] Gramotnev D K and Bozhevolnyi S I 2010 *Nat. Photon.* **4** 83
[2] Wu X F, Zhang J S, Li Z, Liu Y L and Gong Q H 2009 *Chin. Phys. Lett.* **26** 057302
[3] Zhong R B, Liu W H, Zhou J and Liu S G 2012 *Chin. Phys. B* **21** 117303
[4] Chen J J, Li Z, Zhang J S and Gong Q H 2008 *Acta Phys. Sin.* **57** 5893 (in Chinese)
[5] Zhang H F, Cao D, Tao F, Yang X H, Wang Y, Yan X N and Bai L H 2010 *Chin. Phys. Lett.* **19** 027301
[6] Fang Z Y, Thongrattanasiri S, Schlather A, Liu Z, Ma L L, Wang Y M, Ajayan P M, Nordlander P, Halas N J and de Abajo F J G 2013 *ACS Nano* **7** 2388
[7] Zhao J Q, Wang YG, Yan P G, Ruan S C, Cheng J Q, Du G G, Yu Y Q, Zhang G L, Wei H F, Luo J and Tsang Y H 2012 *Chin. Phys. Lett.* **29** 114206
[8] Koppens F H L, Chang D E and de Abajo F J G 2011 *Nano Lett.* **11** 3370
[9] Jablan M, Bujan H and Soljacic M 2009 *Phys. Rev. B* **80** 245435
[10] Li Z Q, Henriksen E A, Jiang Z, Hao Z, Martin M C, Kim P, Stormer H L and Basov D H 2008 *Nat. Phys.* **4** 532
[11] Efetove D K and Kim P 2010 *Phys. Rev. Lett.* **105** 256805
[12] Xia F N, Mueller T, Lin Y M, Valdes-Garcia A and Avouris P 2009 *Nat. Nanotechnol.* **4** 839
[13] Fang Z Y, Wang Y M, Liu Z, Schlather A, Ajayan P M, Koppens F H L, Nordlander P and Halas N J 2012 *ACS Nano* **6** 10222
[14] Xu Y H, Jia Y L, Zhou J and Dong J M 2010 *Chin. Phys. Lett.* **27** 057303
[15] Yang J M, Yang Q, Liu J, Wang Y G and Yuen H T 2013 *Chin. Phys. B* **22** 094210
[16] Schedin F, Lidorikis E, Lombardo A, Kravets V G, Geim A K, Grigorenko A N, Novoselov K S and Ferrari A C 2010 *ACS Nano* **4** 5617
[17] Fang Z Y, Liu Z, Wang Y M, Ajayan P M, Nordlander P and Halas N J 2012 *Nano Lett.* **12** 3808
[18] Nikitin Y, Guinea F, Garcia-Vidal F J and Martin-Moreno L 2011 *Phys. Rev. B* **84** 161407
[19] Ekert K 1991 *Phys. Rev. Lett.* **67** 661
[20] Briegel H J, Dur W, Cirac J I and Zoller P 1998 *Phys. Rev. Lett.* **81** 5932
[21] Christensen J, Manjavacas A, Thongrattanasiri S, Koppens F H L and García de Abajo F J 2012 *ACS Nano* **6** 431
[22] Wunsch B, Stauber T, Sols F and Guinea F 2006 *New J. Phys.* **8** 318
[23] Hwang E H and Sarma S D 2007 *Phys. Rev. B* **75** 205418
[24] Novoselov K S, Geim A K, Morozov S V, Jiang D, Zhang Y, Dubonos S V, Grigorieva I V and Firsov A A 2004 *Science* **306** 666
[25] Novoselov K S, Geim A K, Morozov S V, Jiang D, Katsnelson M I, Grigorieva I V, Dubonos S V and Firsov A A 2005 *Nature* **438** 197
[26] Chen J N, Badioli M, Alonso-Gonzalez P, Thongrattansiri S, Huth F, Osmond J, Spasenovic M, Centeno A, Pesquera A, Godignon P, Elorza AZ, Camara N, Abajo FJG, Hillenbrand R and Koppens F H L 2012 *Nature* **487** 77
[27] Jun Y C, Kekatpure R D, White J S and Brongersma M L 2008 *Phys. Rev. B* **78** 153111